Underwater Visibility Distribution in the Yellow Sea Based on Modis/Aqua Data

Renkui Guo

Ocean University of China, Qingdao 266003, China;

E-mail: guorenkui@126.com

Keywords: Underwater Visibility; MODIS; Attenuation Coefficient; The Yellow Sea

Abstract: Using the data of 2016 in the yellow sea detected by the MODIS sensor on the EOS-Aqua satellite launched by NASA, and using the quantitative relationship between the attenuation coefficient of light passing through a certain sea water and the horizontal visibility of the sea water, the transparency of sea water in different seasons in the yellow sea in 2016 was reflected. The overall results showed that the visibility of seawater in the yellow sea changed significantly with the seasons in 2016, reaching the maximum in summer and the worst in winter.

1. Introduction

In recent years, the study of water color inversion has become a hot topic in ocean remote sensing research, including the observation of ocean transparency, visibility, chlorophyll concentration and other important indicators. The underwater visibility of seawater refers to the underwater visibility, a term borrowed from atmospheric optics[1].Its military activities, Marine research, underwater engineering and other aspects are of great significance.

At the same time, Chinese sea area is large, and has a broad continental shelf and many rivers inflow, the visibility of the size of the space change is very significant. In addition, Chinese sea area is located in the east-Asia and south-Asia monsoon zone, the seasonal variation of visibility is also obvious. Therefore, it is of great significance to monitor the temporal and spatial changes of underwater visibility in Chinese sea areas.

During the second world war, foreign countries began to study the visibility of sea water[2]. From the second world war to the mid-1970s, some countries studied the visibility of sea water mainly for military security and underwater engineering. For example, the port of San Diego in the United States[3] uses the visibility distribution in water to monitor the security around the port, which is used to prevent terrorist organizations from launching terrorist attacks, and to monitor divers, submarines and other equipment of terrorist organizations under the sea water. In addition, Martin Roser[4] et al. proposed a new underwater image enhancement method to enhance underwater visibility, and applied this method to autonomous underwater vehicles to improve their performance. Gal Oren[5] proposed a method for underwater robot motion planning based on visibility, and tested it in a challenge scenario demonstrating safety trajectory planning. Sattar j.[6] et al. studied the performance of different algorithms applied to visual target tracking technology when the visibility decreases due to the changes of light and suspended particles in the Marine environment. Beilei Hu[7] et al. proposed a new method to realize underwater image color correction, which solved the problems of backscatter noise and color degradation in low-visibility underwater vision.

There are a lot of research results in the field of visibility in China, especially atmospheric visibility, which is often involved in the field of meteorology. However, there is no research report on the monitoring of seawater visibility parameters, which is only involved in the seawater transparency[8].For example, Wang Xiaofei[9] et al. established the transparency remote sensing inversion model of the northwest Pacific Ocean by using the remote sensing reflectivity and transparency data measured in the field, and applied it to the Seawifs, MODIS-aqua, MODIS-terra and MERIS Level 2 reflectivity data to obtain the transparency data of the northwest Pacific Ocean. Gao lei[10] et al. analyzed the temporal and spatial distribution of seawater transparency based on 2014 Marine monitoring data in the coastal waters of Qingdao. But transparency is the vertical

Copyright © (2019) Francis Academic Press, UK DOI: 10.25236/csam.2019.062

depth of looking down on the water, and visibility is the horizontal distance you can see in the water. Therefore, the research on sea water visibility in China is basically blank.

2. Data and methods

Satellite data inversion refers to the method of obtaining Marine environmental parameters from the original satellite data, that is, the inverse operation from the electromagnetic field to the physical or geophysical properties. The inversion on remote sensing is based on model knowledge, and the state parameters of the target are derived from the values of measurable parameters. In other words, according to the observation information and forward physical model, the application parameters describing the ground reality can be solved or calculated. Ocean water color remote sensing USES airborne or spaceborne remote sensing to detect spectral radiation of parameters related to ocean water color. There are two key technologies to obtain the information of ocean water color elements from the water color satellite data. One is atmospheric correction, that is, to eliminate the influence of the atmosphere from the signals received by the sensor, and to obtain the brightness of sea surface radiance containing the information of sea water components. The other is the bioluminescence algorithm, that is, according to the optical characteristics of different sea water and the brightness of the radiance from the water, to estimate the relevant Marine color elements.

In recent years, the variety of water-color satellite products in China has become increasingly rich and comprehensive, covering all the research data of water-color remote sensing related bands from ultraviolet to medium and long wave infrared[11]. However, as far as the present stage is concerned, MODIS is the most commonly used water-color remote sensing data in China. China has established MODIS national data center in 2003, which is responsible for the long-term security storage, management, development, and sharing of MODIS data[12].

The Moderate Resolution Imaging Spectro-Radiometer[13] is one of the primary sensors on NASA's earth observation satellites, eos-terra and eos-aqua. It has a wide range of data bands, reaching 36 bands and a higher temporal resolution. The spatial resolution of data includes 250 meters, 500 meters and 1000 meters, which is conducive to capturing the dynamic change information of the ground.

In this paper, the data of Modis sensor on Aqua satellite are used for inversion calculation of underwater visibility in the yellow sea region in 2016 and analysis of its characteristics in different seasons.Since the remote sensing reflectivity is used to calculate the underwater visibility in this paper, only the level 2 OC type data containing remote sensing reflectivity data need to be downloaded[14].In the above range of data, select the data covering the yellow sea for research.After getting the data, the atmospheric correction processing of the data row is conducted with SEADAS first, so as to eliminate the influence of atmospheric aerosols in the original data, and then the subsequent inversion step is carried out[15].

In the process of data inversion, the surface remote sensing reflectance R_{rs} refers to the ratio of out-of-water radiance to downward irradiance E_d, while r_{rs} refers to the ratio of out-of-water radiance to upward irradiance E_d.

According to relevant literature[16], the relationship between the two is:

$$r_{rs}(\lambda)=\frac{R_{rs}(\lambda)}{0.52+1.7R_{rs}(\lambda)}$$

$a(\lambda)$ refers to the absorption coefficient of seawater with wavelength λ. According to literature[17], it can be seen that:

$a(440)=10^{-0.619-1.969\rho+0.79\rho^2}$,where $\rho=\log_{10}\left[\frac{r_{rs}(490)}{r_{rs}(555)}\right]$

$b_{bp}(\lambda)$ refers to the backscattering coefficient of particles in seawater against light of

wavelength λ,

$b_{bp}(440)=\frac{u(440)a(440)}{1-u(440)}-b_{bw}(440)$, $b_{bp}(\lambda)=b_{bp}(440)\left(\frac{440}{\lambda}\right)^{Y}$,

$Y=2.2\left\{1-1.2e^{-0.9\left[\frac{r_{rs}(490)}{r_{rs}(555)}\right]}\right\}$, $u(\lambda)=\frac{-g_0+\left[(g_0)^2+4g_1r_{rs}(\lambda)\right]^{\frac{1}{2}}}{2g_1}$

where

According to literature[15], it can be seen that:

g_0=0.0895, g_1=0.1247,

$b_b(\lambda)$ refers to the backscattering coefficient of seawater against light of wavelength λ, and b_{bw} is the backscattering coefficient of pure water against light of wavelength λ,

$b_b(\lambda)=b_{bp}(\lambda)+b_{bw}(\lambda)$,

According to $u(\lambda)=\frac{b_b(\lambda)}{a(\lambda)+b_b(\lambda)}$, we can deduce $a(\lambda)$,

According to $a(\lambda)=a_{pg}(\lambda)+a_w(\lambda)$, we can deduce $a_{pg}(\lambda)$,

Where $a_w(\lambda)$ is the absorption coefficient of pure water to wavelength λ,

$a_{pg}(\lambda)$ refers to the sum of absorption coefficients of particles and yellow substances in seawater with wavelength λ,

namely $a_{pg}(\lambda)=a_p(\lambda)+a_g(\lambda)$,

$b_p(\lambda)$ refers to the scattering coefficient of particles in seawater to light of wavelength λ,

$b_{bp}(\lambda)=0.0183b_p(\lambda)$, we can deduce $b_p(\lambda)$,

In addition, $c_{pg}(\lambda)=a_{pg}(\lambda)+b_p(\lambda)$,

Attenuation coefficient $\alpha=0.9c_{pg}(\lambda)+0.081$,

y means horizontal visibility. According to literature[2], it can be seen that: $y=\frac{4.8}{\alpha}$.

Based on the above quasi-analytical method, the attenuation coefficient of light with a wavelength of λ in seawater can be derived, where the wavelength is 532nm channel light, and finally the visibility can be obtained.

3. Results and Analysis

As shown in figure 1, in general, the underwater visibility of the yellow sea is relatively low in winter. Under the influence of atmospheric pressure activities, the yellow sea area has strong wind force and the concentration of suspended matter in seawater increases, so the visibility in winter is generally low. The visibility in the yellow sea is basically less than 20m in a wide range. At the mountain corner of the Shandong peninsula, there is an ear-shaped water tongue with low visibility, and the visibility is less than 5m. The content of suspended matter in north Jiangsu shoal is high all year round and the visibility is very low. Meanwhile, due to the influence of ocean currents, the visibility in the east of the yellow sea is also low, only 5-6m.In winter, visibility in the south yellow sea is the lowest in a year.

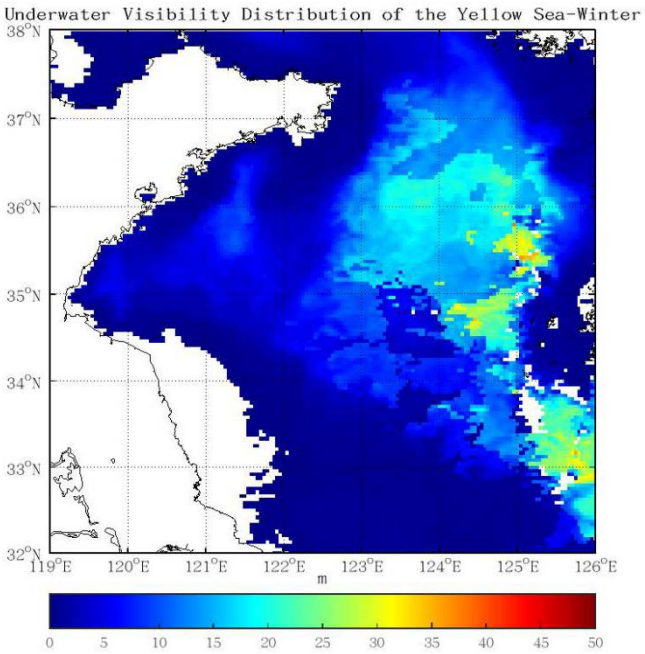

Fig.1. Underwater visibility distribution of the yellow sea in the winter of 2016

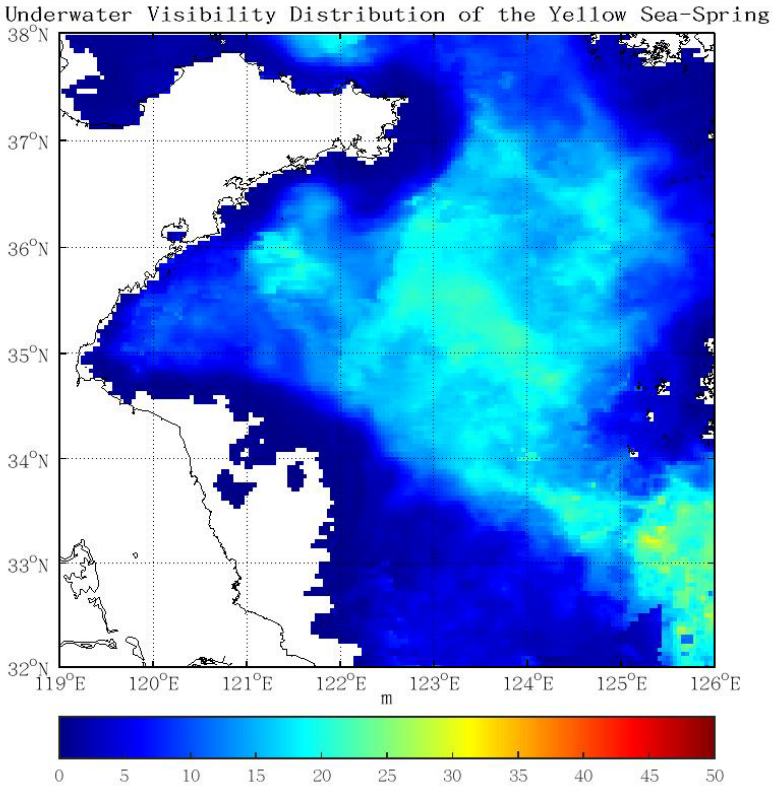

Fig.2. Underwater visibility distribution of the yellow sea in the spring of 2016

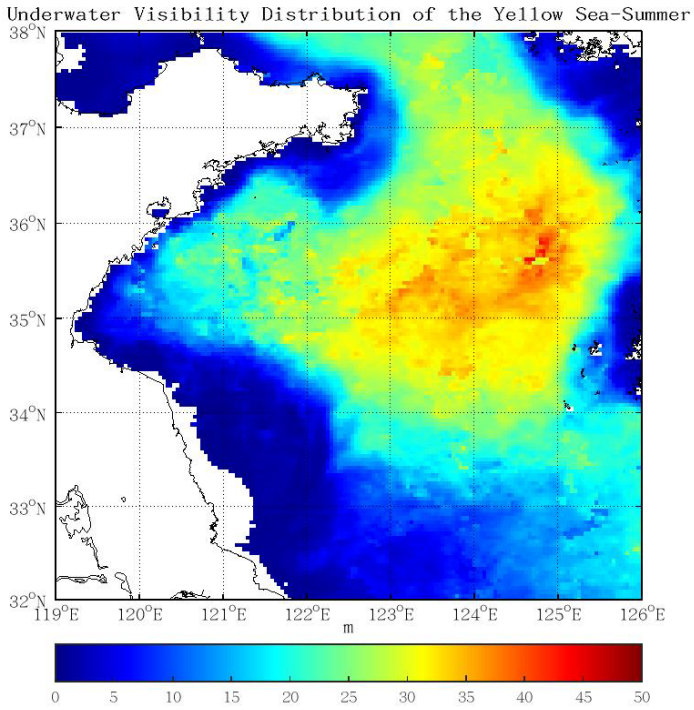

Fig.3. Underwater visibility distribution of the yellow sea in the summer of 2016

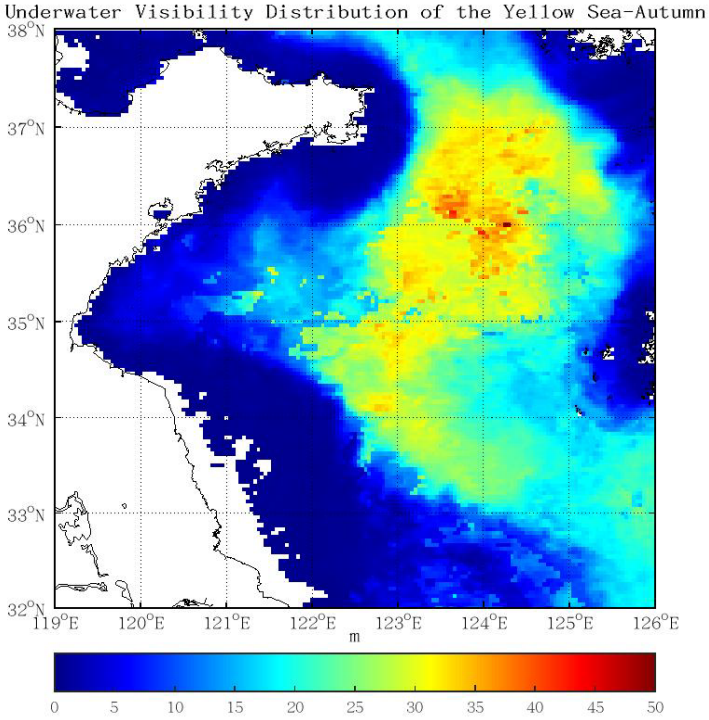

Fig.4. Underwater visibility distribution of the yellow sea in the autumn of 2016

Spring is the transition period from winter monsoon to summer monsoon. The water temperature in the yellow sea rises and plankton grows rapidly. At this time, the visibility of seawater is still low, as shown in figure 2. Visibility in the shallow waters of the continental shelf increased significantly than in winter. The scope of the ear-shaped low-visibility waters at the mountain corner was gradually narrowed, and the scope of the low-visibility waters east of the north Jiangsu shoal was also gradually narrowed. In particular, compared with the sea area of Lianyungang, this area shrank to the west by about 3 longitude degrees. There is also a tendency for the low-visibility zone on the west coast of the Korean peninsula to retreat to the shore. The visibility in the north yellow sea increases gradually, but it is still at a low value, with an average size of about 10-20m. The visibility

in the central region of the south yellow sea is about 20-30m on average.

In summer, the southwest wind prevails in the yellow sea area, with low wind speed and high water temperature. The seawater generates thermocline, and the visibility in the yellow sea area increases, especially in the strong and prosperous period of the thermocline. Therefore, the yellow sea has the highest visibility in summer, as shown in figure 3.The visibility in the north yellow sea increased rapidly in summer. The high visibility water was like a tongue extending from the east to the west into the Bohai sea. The visibility was more than 30m.The area of ear-shaped low-visibility waters near the mountain corner of the Shandong peninsula was reduced to the lowest in the whole year, and the area of low-visibility waters east of the shoal of north Jiangsu was also reduced to the lowest in the whole year. Visibility near the Korean peninsula was the highest of the year. In the southern part of the yellow sea, far away from land, visibility also increases rapidly, reaching an average of 30-40m.

Autumn is the transition period from summer monsoon to winter monsoon, and the plankton reaches the weak peak in a year [19]. Visibility in the yellow sea decreased from that in summer, but remained high. In the northern part of the yellow sea, the transition from summer to winter is rapid, the water temperature decreases, and the seasonal thermocline disappears quickly. The visibility of the waters in the middle and northern part of the yellow sea began to decrease. The area of low visibility in the north shoal of Jiangsu spreads eastward, and the area of ear-shaped low visibility in the mountain corner gradually expands. The area of low-visibility waters near the Korean peninsula also gradually increased, and the visibility in the southern waters of the yellow sea also gradually decreased. The visibility in the central region was about 25m on average, as shown in figure 4.

It can be seen from the above analysis that the visibility of the yellow sea area changes significantly with the seasons and the geographical distribution is also different. The visibility was lower in winter and spring and higher in summer and autumn. The general trend with regional changes is that the visibility is high away from the land and sea, and low in the shoal area close to the land, which changes layer by layer.

References

[1] FENG Shi-Zuo, LI Feng-Qi, LI Shao-Jing. Introduction to Marine science. Higher Education Press, 1999.372-388

[2] J.Ronald V.Zaneveld, W.Scott Pegau. Robust underwater visibility parameter. OPTICS EXPRESS, 2003, Vol. 11, No. 23:2997-3009

[3] Charles C.Trees, Paul W.Bissett, Heidi Dierssen, David D.R.Kohler, Mark A.Moline, James L.Mueller, Richard E.Pieper, Michael S.Twardowski, J.Ronald V.Zaneveld.Monitoring water transparency and diver visibility in ports and harbors using aircraft hyperspectral remote sensing. Proceedings of SPIE, Vol. 5780:91-98

[4] Roser M, Dunbabin M , Geiger A . Simultaneous underwater visibility assessment, enhancement and improved stereo[C]// IEEE International Conference on Robotics & Automation. IEEE, 2014.

[5] Gal O. Visibility-Based Path Planning for Autonomous Underwater Vehicle[C]// Robotics; Robotik ; German Conference on. VDE, 2012.

[6] Sattar J , Dudek G . [IEEE 2006 IEEE International Conference on Robotics and Automation, 2006. ICRA 2006. - Orlando, FL, USA (May 15-19, 2006)] Proceedings 2006 IEEE International Conference on Robotics and Automation, 2006. ICRA 2006. - On the performance of color tracking algorithms for underwater robots under varying lighting and visibility[C]// Robotics and Automation, 2006. ICRA 2006. Proceedings 2006 IEEE International Conference on. IEEE, 2006:3550-3555.

[7] Hu B , Zheng B , Yang Y , et al. Underwater image color correct in extremely poor visibility[C]// Oceans. IEEE, 2014.

[8] ZHAO Jun, DAI Wen-hao. Remote sensing inversion of ocean water color and transparency

using MODIS data. Chemical Engineering & Equipment, 2008(9):47-48

[9] WANG Xiao-Fei, ZHANG Ting-Lu, TIAN Lin, SHI Ying-Ni. Secchi Disk Depth Retrieval and Merging in the Northwest Pacific from Multiple Missions of Ocean Color Remote Sensing. Periodical of Ocean University of China, 2016,46(12):133-141.

[10] GAO Lei, YAO Hai-yan, ZHANG Meng-meng, et al. Temporal and spatial variation of seawater transparency and its relationship with environmental factors in Qingdao coastal area[J]. Journal of Marine Sciences, 2017, 35(3) : 79-84,doi: 10.3969/j. issn. 1001-909X.2017.03. 009.

[11] ZHANG Ke-Li, BAI Zhao-Guang, WANG Li-Li. Review, present situation and prospect of Marine color satellite development in China[J]. Satellite Application, 2018(05):24-27

[12] CHE Zhi-sheng. Ocean Color Satellite Development in China[J]. Journal of Guangxi Academy of Sciences, 2009,25(01):76-80

[13] LIU Yu-Jie, YANG Zhong-Dong. MODIS remote sensing information processing principle and algorithm. Science Press, 2001.1-3

[14] MODIS Website. Ocean level 2 data products. March,22 2010.

http://oceancolor.gsfc.nasa.gov/DOCS/Ocean_Level-2_Data_Products.pdf

[15] YUAN Yuan, XU Hui-Ping. MODIS data preprocessing based on sea color remote sensing application[J]. Geospatial Information, 2014,12(01):93-95+11

[16] ZhongPing Lee,Kendall L.Carder,Robert A.Arnone. Deriving inherent optical properties from water color: a multiband quasi-analytical algorithm for optically deep waters. APPLIED OPTICS,2002,Vol. 41,No. 27:5755-5772.

[17] ZhongPing Lee,Kendall L.Carder. An empirical algorithm for light absorption by ocean water based on color. Journal of Geophysical Research,1998,Vol.103,No.C12 : 27967–27978

[18] HU Hao-guo, WAN Zhen-wen, YUAN Ye-li. Simulation of seasonal variation of phytOplanktOn in the southern Huanghai (Yellow) Sea and analysis on its influential factors. ACTA OCEANOLOGICA SINICA, 2004, 26(4): 74-88

[19] GAO Shuang, LI Zheng-Yan. Spatial and Seasonal Variation of Chlorophyll and Primary Productivity in Summer and Winter in the Northern Yellow Sea. PERIODICAL OF OCEAN UNIVERSITY OF CHINA, 2009, 39(4): 604-610